N-channel transparent organic thin-film transistors with Ag/LiF bilayer transparent source–drain electrodes fabricated by thermal evaporation

2014 Appl. Phys. Express 7 021601

(http://iopscience.iop.org/1882-0786/7/2/021601)

Applied Physics Express 7, 021601 (2014)
http://dx.doi.org/10.7567/APEX.7.021601

N-channel transparent organic thin-film transistors with Ag/LiF bilayer transparent source–drain electrodes fabricated by thermal evaporation

Nan Zhang[1,2], Jie Lin[1], Jinsong Luo[1], Yantao Li[1], Zhihong Gan[1], Yi Fan[1]*, and Xingyuan Liu[1]*

[1]State Key Laboratory of Luminescence and Applications, Changchun Institute of Optics, Fine Mechanics and Physics, Chinese Academy of Sciences, Changchun 130033, China
[2]University of Chinese Academy of Sciences, Beijing 100049, China
E-mail: liuxy@ciomp.ac.cn; fanyi@ciomp.ac.cn

Received December 3, 2013; accepted December 18, 2013; published online January 14, 2014

In this paper, we report the use of Ag/LiF (AL) bilayer transparent source–drain (S/D) electrodes for n-channel F_{16}CuPc-based transparent organic thin-film transistors (OTFTs). The transparent electrodes are deposited at room temperature by thermal evaporation, with devices subsequently fabricated without damaging the active layer or breaking the vacuum. Consequently, we obtain transparent OTFTs based on AL bilayer transparent S/D electrodes with good electron mobility of $1.31 \times 10^{-2}\,cm^{-2}{\cdot}V^{-1}{\cdot}s^{-1}$, a high on/off ratio of 4.2×10^6, and an average visible range transmittance of 55.6%.

Transparent organic thin-film transistors (OTFTs) have received considerable attention recently owing to their potential applications in transparent flexible electronic devices.[1)] Previous studies have also shown a favorable mobility with transparent OTFTs compared with conventional amorphous silicon (a-Si) TFTs.[2)] To date, most transparent OTFTs have been p-channel devices in which the channel carrier is a hole. There have been few reports regarding n-channel or ambipolar transparent OTFTs. To develop transparent organic electronics, p-channel and n-channel transistors should ideally be combined to produce low-power circuits, such as silicon-based integrated circuits (ICs). For transparent OTFTs, various transparent conductive films including poly(ethylene dioxythiophene):poly(styrene sulfonate) (PEDOT:PSS),[3)] indium tin oxide (ITO),[4)] Al:ZnO (AZO),[5)] NiO_x,[6)] carbon nanotubes,[7)] graphene,[8)] and reduced graphene oxide[9)] have all been used as source–drain (S/D) electrodes. However, their fabrication processes and properties have so far proven to be far from satisfactory. They can therefore have a severe negative impact on the performance of transparent OTFTs, particularly with regard to sputter damage of the active organic semiconductor layer. Furthermore, the lag in the advancement of n-channel common/transparent OTFTs can also be attributed to the large electron injection barrier between the work function of common metal/transparent electrodes and the lowest unoccupied molecular orbital (LUMO) of the n-type organic semiconductor.[10)] Therefore, the key to transparent organic logic circuits is the realization of n-channel transparent OTFTs based on transparent S/D electrodes, with a proper fabrication process and good optical-electrical properties.

According to previous studies, transparent electrodes based on metal–dielectric (MD) or dielectric–metal–dielectric (DMD) structures can achieve enhanced transmittance in a selective region via the interference effect.[11–13)] These transparent electrodes have been used in organic/inorganic optoelectronic devices and are capable of obtaining high device performance.[11–13)] However, detailed research into bilayer or trilayer transparent electrodes for n-channel transparent OTFTs has not yet been reported. In general, the optical performance of a bilayer structure is lower than that of a trilayer structure, as the transmission of a trilayer is more easily optimized. However, in terms of organic layer/electrode interface contact performance, a bilayer MD structure would be preferable to a trilayer DMD structure, provided the dielectric layer has a poor conductive performance. In this letter, we report on n-channel transparent OTFTs based on Ag/lithium fluoride (LiF) bilayer transparent S/D electrodes. The Ag/LiF (AL) transparent electrodes were deposited at room temperature by thermal evaporation, which is a fabrication process compatible with organic devices as it does not damage the active organic layer. Additionally, the devices could be fabricated without the need for breaking the vacuum. After simulation and experimentation, the structure of the AL transparent electrodes was confirmed to have good electrical and optical properties. N-channel transparent OTFTs with AL electrodes demonstrate a good electron mobility of $1.31 \times 10^{-2}\,cm^{-2}{\cdot}V^{-1}{\cdot}s^{-1}$, a high on/off ratio of 4.2×10^6, and an average visible range transmittance of 55.6%. To the best of our knowledge, this is the first time that n-channel transparent OTFTs based on bilayer transparent electrodes have been achieved.

The AL transparent electrodes were deposited on glass substrates that had been ultrasonically cleaned with acetone, ethanol, and deionized water prior to use. LiF and Ag films were prepared by thermal evaporation at room temperature under a vacuum pressure of 1.7×10^{-4} Pa. The evaporation rates of LiF and Ag were 0.1 and 1 nm/s, respectively. In this particular study, hexadecafluorophthalocyaninatocopper (F_{16}CuPc) was selected as the active organic semiconductor layer. F_{16}CuPc, along with polystyrene (PS), poly(4-vinylphenol) (PVP), poly(melamine-*co*-formaldehyde), and propylene glycol monomethyl ether acetate (PGMEA), were all purchased from Sigma-Aldrich and used without further treatment. The ITO gate electrodes were patterned by photolithography and wet etching, with the ITO glass substrates then ultrasonically cleaned with acetone, ethanol, and deionized water in sequence. An organic dielectric layer of PVP was prepared by spin coating it in PGMEA, and then annealed at 180 °C for 1 h in a glove box to create a 600-nm-thick PVP layer. Since hydroxyl groups on the PVP surface can act as electron traps and reduce the electron mobility,[14)] they were removed by modifying the PVP dielectric layer surface with a 6 mg/ml solution of PS in anhydrous toluene ($M_W = 280{,}000$). After spin-coating at 2000 rpm for 30 s, the substrate was cured in a glove box at 120 °C for 1 h. Next, a 30-nm-thick film of F_{16}CuPc was deposited at room temperature by thermal evaporation, using a shadow mask to

achieve the desired patterning. The evaporation rate of $F_{16}CuPc$ was controlled at 0.2 nm/s under a vacuum of 1.5×10^{-4} Pa. Finally, the sample was transferred to another chamber without breaking the vacuum, with the transparent S/D electrodes then being deposited on the active layer through a shadow mask with a channel length and width of 100 μm and 3 mm, respectively. The film thicknesses were measured with an Ambios XP-1 surface profiler. The work function of the AL electrode was measured using a KP Technology Ambient Kelvin probe system package. The electrical characteristics of the OTFTs were determined with a Keithley 4200 SCS semiconductor characterization system. The optical transmittance spectra were measured with a Shimadzu UV-3101PC spectrophotometer. All the samples for transmittance measurements were of the same 18×18 mm^2 dimensions, creating an area of incident light of about 4 mm^2. All measurements were performed in air ambient without any encapsulation.

To optimize the optical transmittance of the transparent electrodes, the transmittances of the AL structures were calculated by the optical transfer matrix method.[11,15,16] Figure 1(a) shows the calculated contour plots for the transmittance of the AL structures at 550 nm as a function of the Ag and LiF layer thicknesses. The specific details of this calculation method are shown in a previous study.[16] When the LiF thickness is greater than 20 nm, the transmittance of the AL electrode is dependent on the thickness of the Ag layer. The transmittance can therefore be optimized to over 90%, with particularly good transmittances obtained with a Ag layer thickness varying from 4 to 12 nm when the LiF layer thickness is greater than 20 nm. The measured transmittance spectra of separate AL samples with different structures are shown in Fig. 1(b). The difference observed between the simulated and experimental data may have resulted from a change in the optical constants of Ag and LiF layers during the deposition.

With regard to the electrical properties of the AL structure, Fig. 1(c) shows that there is a marked decrease in sheet resistance from 63 to 5 Ω/sq with an increase in the Ag layer thickness. This sheet resistance was measured by a four-point probe method with a surface resistivity meter, with the probe in direct contact with the surface of the LiF layer. Those AL transparent electrodes having a Ag layer thickness of more than 10 nm show a lower sheet resistance, because of the continuous film growth of the Ag layer.[11,12] This indicates that the Ag layer thickness determines the electrical properties of the AL electrodes. The simulation and experimental data confirm that AL transparent electrodes (10/70 nm) possess good optical-electrical properties, thus making them suitable for use in transparent OTFTs.

A schematic diagram of the transparent OTFT structure is shown in Fig. 2(a), in which the Ag layer was in direct contact with the $F_{16}CuPc$ channel layer. Figures 2(b) and 2(c) show the transmittance spectra of devices with an increasing number of individual layers, both with and without transparent S/D electrodes. All samples in Figs. 2(b) and 2(c) were formed on the same 18×18 mm^2 substrate, which was fully covered by the film to facilitate the transmittance measurement. After the transmittance measurement of the glass/ITO sample was recorded, a layer of PVP was formed on top and the transmittance of the new glass/ITO/PVP

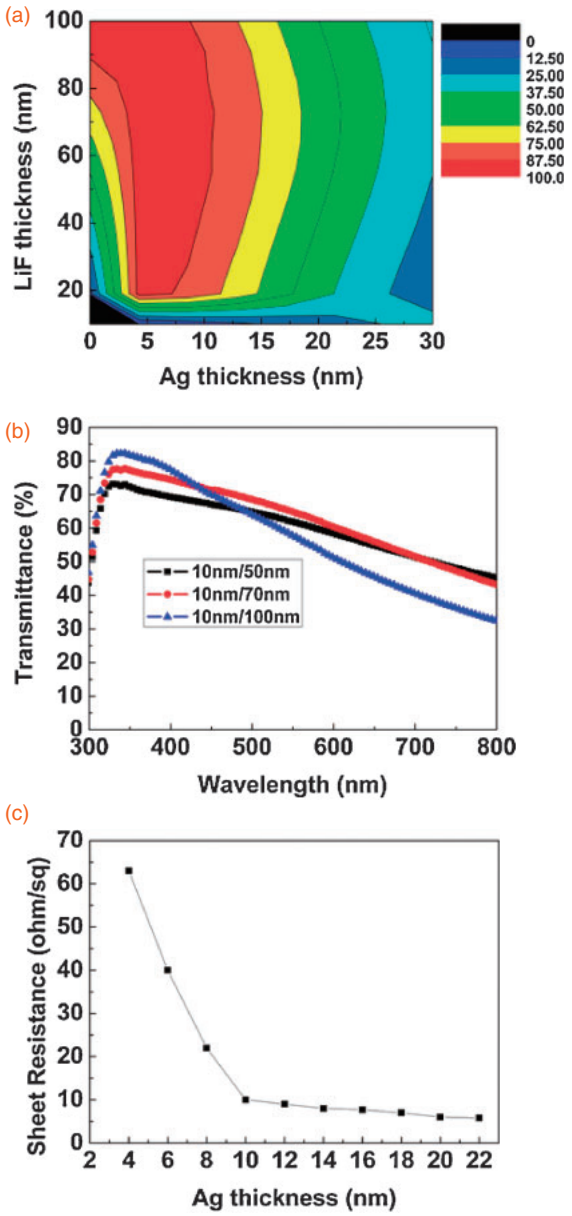

Fig. 1. (a) Calculated transmittance of the Ag/LiF structure at a wavelength of 550 nm as a function of Ag and LiF layer thicknesses. (b) Measured transmittance spectra of different Ag/LiF structures. (c) Sheet resistance of the Ag/LiF electrodes as a function of the Ag layer thickness. The thickness of the LiF layer is fixed at 70 nm.

sample was then determined. Additional layers were prepared and tested by the same method. The transmittances of the samples between 300 and 900 nm decreased slightly when the individual layers were stacked sequentially from the ITO gate electrode layer to the active organic semiconductor layer ($F_{16}CuPc$). In Fig. 2(b), the absorption peak observed near 630 and 800 nm is related to the orbital gap of $F_{16}CuPc$ between the highest occupied molecular orbital (HOMO) and LUMO.[17–19] The average transmittance of the device with AL transparent electrodes is higher in the visible range (from 400 to 750 nm) than that of a device with only Ag electrodes, suggesting that the use of a thermally evaporated LiF layer as an index-matching layer can increase the device transmittance. Figure 2(d) shows a photograph of a four-device array, with the regions identified by black arrows (i) and (ii) representing devices with and without an organic active layer

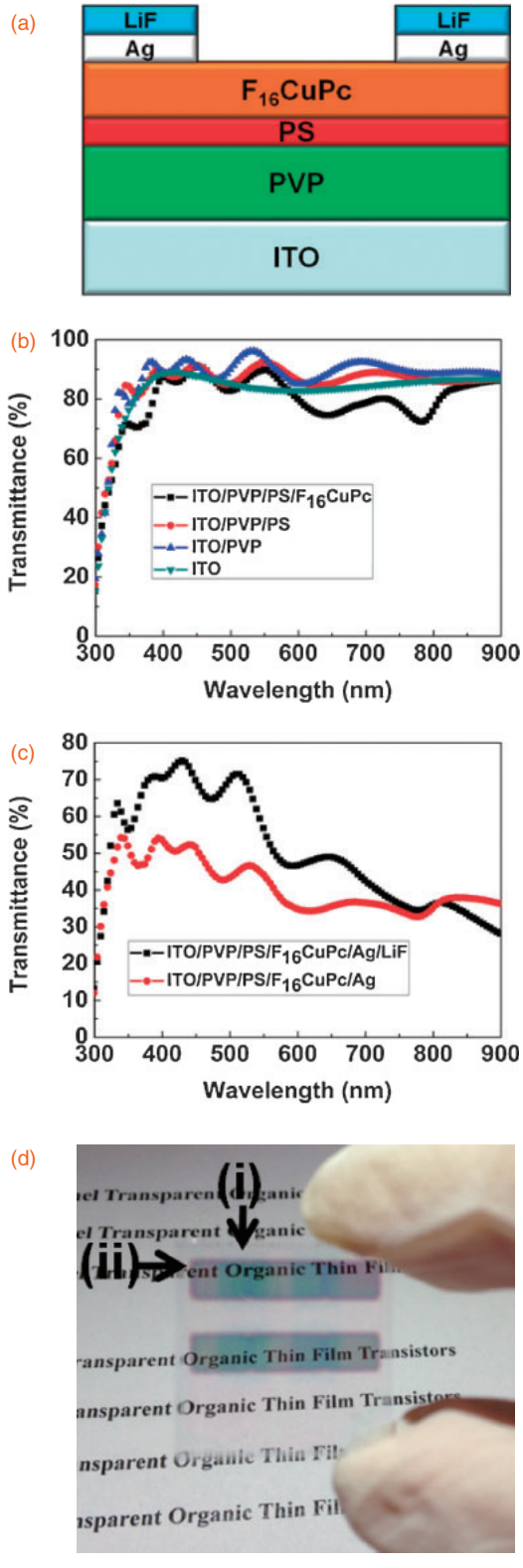

Fig. 2. (a) Schematic diagram of the transparent OTFT structure. (b) Transmittance spectra of the transparent device with increasing stacking of layers from the ITO gate electrodes to the $F_{16}CuPc$ active layer. (c) Transmittance spectra of the transparent device with Ag and Ag/LiF. (d) Photograph of a four-device array. Inset: The regions identified by black arrows (i) and (ii) are devices with and without an organic active layer ($F_{16}CuPc$), respectively.

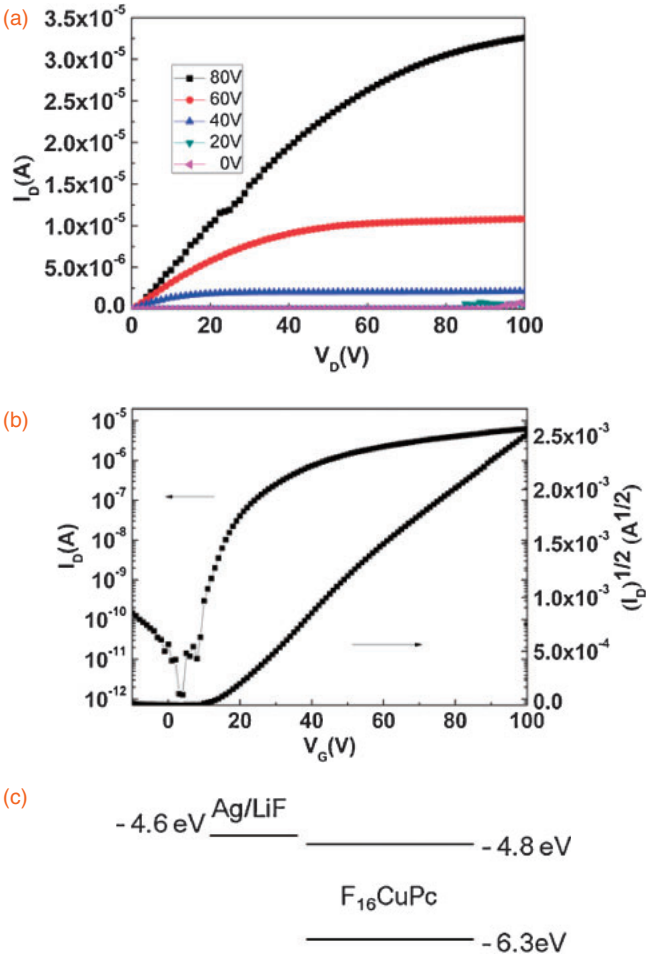

Fig. 3. (a) Output characteristics of OTFTs with Ag/LiF S/D electrodes. $V_G = 0$–80 V. (b) Transfer characteristics of OTFT with Ag/LiF S/D electrodes at $V_D = 20$ V. (c) Energy diagram of the AL/$F_{16}CuPc$ interface.

($F_{16}CuPc$), respectively. The average transmittance of this device is 55.6%, and thus a semitransparent device has been successfully achieved. Furthermore, these devices are expected to become more transparent as the structure is further optimized.

Figures 3(a) and 3(b) show the typical output and transfer characteristics of transparent OTFTs with AL transparent S/D electrodes. The output characteristics shown in Fig. 3(a) demonstrate clear linear and saturation regimes, which indicate that the devices operate in an n-type accumulation mode. The carrier mobility is calculated in the saturation regime using the following formula:

$$I_D = \mu C_i \left(\frac{W}{2L}\right)(V_G - V_T)^2, \quad (1)$$

where I_D, C_i, μ, V_G, V_T, W, and L are the drain current, capacitance per unit area of the gate dielectric, carrier mobility, gate voltage, threshold voltage, channel width, and channel length, respectively. The electron mobility of $F_{16}CuPc$-based OTFTs with AL transparent S/D electrodes is $1.31 \times 10^{-2}\,cm^{-2}\cdot V^{-1}\cdot s^{-1}$ (see Table I), which is comparable to that of OTFTs with a $F_{16}CuPc$ semiconductor active layer.[20–22] It was reported by Cosseddu et al. that ambipolar OTFTs possess very poor n-type behavior, owing to an electron injection barrier of approximately 1.5 eV.[3] The work function of the Ag/LiF bilayer electrode measured from the metal Ag side is about −4.6 eV. As shown in Fig. 3(c), a very small energy gap of 0.2 eV (close to ohmic contact) exists

Table I. Electrical properties of Ag/LiF. Device performance for F_{16}CuPc-based OTFTs with Ag/LiF S/D electrodes.

Structure (nm)	10/70
Sheet resistance (Ω/sq)	10
Resistivity (Ω·cm)	6×10^{-5}
Device electron mobility ($cm^{-2}\cdot V^{-1}\cdot s^{-1}$)	1.31×10^{-2}
Device on/off ratio	4.2×10^{6}

between F_{16}CuPc and AL electrodes, which contributes to the high device performance. Thus, the AL bilayer transparent electrodes have a low sheet resistance, good transmittance, and a favorable work function. They can also be deposited at room temperature with little damage to the organic active layer, and produce good device performance when used as transparent S/D electrodes in F_{16}CuPc-based OTFTs.

In conclusion, Ag/LiF bilayer transparent S/D electrodes have been proven effective for n-channel F_{16}CuPc-based transparent OTFTs. These transparent electrodes were deposited at room temperature by thermal evaporation, with devices being fabricated without causing damage to the active organic layer or breaking the vacuum. The n-channel transparent OTFTs exhibited a good electron mobility of 1.31×10^{-2} $cm^{-2}\cdot V^{-1}\cdot s^{-1}$, a high on/off ratio of 4.2×10^{6}, and an average visible range transmittance of 55.6%. This study reveals that AL transparent electrodes are an excellent choice for n-channel transparent OTFTs, and that these OTFTs have the potential for use in transparent organic logic ICs.

Acknowledgments This work is supported by the CAS Innovation Program, and National Science Foundation of China Nos. 51102228 and 61106057.

1) S.-J. Kim, J.-M. Song, and J.-S. Lee, J. Mater. Chem. **21**, 14516 (2011).
2) X. Qian, T. Wang, and D. Yan, Org. Electron. **14**, 1052 (2013).
3) P. Cosseddu, A. Bonfiglio, I. Salzmann, J. P. Rabe, and N. Koch, Org. Electron. **9**, 191 (2008).
4) H. Ohta, T. Kambayashi, K. Nomura, M. Hirano, K. Ishikawa, H. Takezoe, and H. Hosono, Adv. Mater. **16**, 312 (2004).
5) D.-J. Yun and S.-W. Rhee, Thin Solid Films **517**, 4644 (2009).
6) J.-M. Choi, D. K. Hwang, J. H. Kim, and S. Im, Appl. Phys. Lett. **86**, 123505 (2005).
7) Q. Cao, Z.-T. Zhu, M. G. Lemaitre, M.-G. Xia, M. Shim, and J. A. Rogers, Appl. Phys. Lett. **88**, 113511 (2006).
8) W. H. Lee, J. Park, S. H. Sim, S. B. Jo, K. S. Kim, B. H. Hong, and K. Cho, Adv. Mater. **23**, 1752 (2011).
9) K. Suganuma, S. Watanabe, T. Gotou, and K. Ueno, Appl. Phys. Express **4**, 021603 (2011).
10) Q. Meng and W. Hu, Phys. Chem. Chem. Phys. **14**, 14152 (2012).
11) X. Guo, J. Lin, H. Chen, X. Zhang, Y. Fan, J. Luo, and X. Liu, J. Mater. Chem. **22**, 17176 (2012).
12) K. Hong, K. Kim, S. Kim, I. Lee, H. Cho, S. Yoo, H. W. Choi, N.-Y. Lee, Y.-H. Tak, and J.-L. Lee, J. Phys. Chem. C **115**, 3453 (2011).
13) K.-H. Choi, H.-W. Koo, T.-W. Kim, and H.-K. Kim, Appl. Phys. Lett. **100**, 263505 (2012).
14) L.-L. Chua, J. Zaumseil, J.-F. Chang, E. C.-W. Ou, P. K.-H. Ho, H. Sirringhaus, and R. H. Friend, Nature **434**, 194 (2005).
15) X. Liu, X. Cai, J. Qiao, J. Mao, and N. Jiang, Thin Solid Films **441**, 200 (2003).
16) C. Song, H. Chen, Y. Fan, J. Luo, X. Guo, and X. Liu, Appl. Phys. Express **5**, 041102 (2012).
17) C. Videlot-Ackermann, J. Ackermann, and F. Fages, Synth. Met. **157**, 551 (2007).
18) J. L. Yang, S. Schumann, R. A. Hatton, and T. S. Jones, Org. Electron. **11**, 1399 (2010).
19) M. Gorgoi, W. Michaelis, T. U. Kampen, D. Schlettwein, and D. R. T. Zahn, Appl. Surf. Sci. **234**, 138 (2004).
20) Z. Bao, A. J. Lovinger, and J. Brown, J. Am. Chem. Soc. **120**, 207 (1998).
21) R. Ye, M. Baba, K. Suzuki, and K. Mori, Thin Solid Films **517**, 3001 (2009).
22) C. Keil and D. Schlettwein, Org. Electron. **12**, 1376 (2011).